Sustainable Production of Potato Pulp-derived Cellulose Nanocrystals with Enhanced Heavy Metal Adsorption and Biocompatibility: A Comparative Study with Conventional Feedstocks

Fahimeh Mohammadpanah [a], Rabi Behrooz [a,*], Mahsa Pooyan [b], and Roohollah Roohzadeh [b,c]

*Corresponding author: Rabi.Behrooz@modares.ac.ir

DOI: 10.15376/biores.21.2.2851-2877

Graphical Abstract

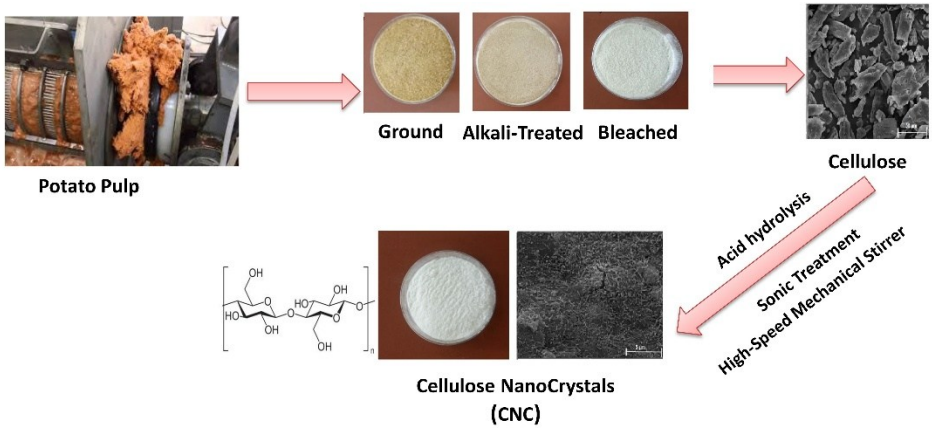

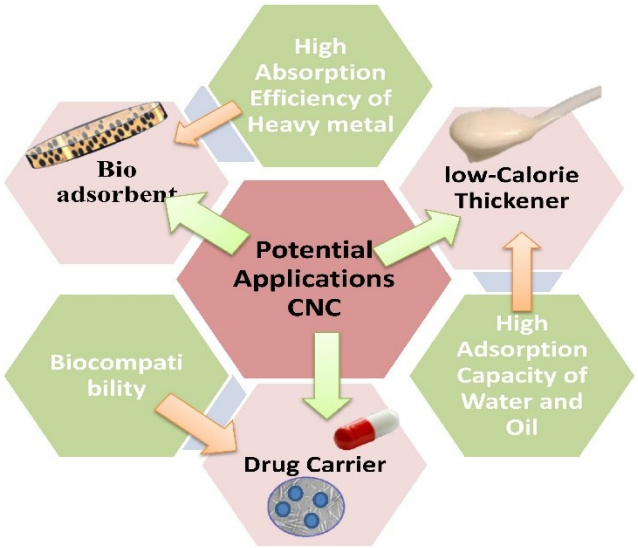

Sustainable Production of Potato Pulp-derived Cellulose Nanocrystals with Enhanced Heavy Metal Adsorption and Biocompatibility: A Comparative Study with Conventional Feedstocks

Fahimeh Mohammadpanah [a], Rabi Behrooz [a,*], Mahsa Pooyan [b], and Roohollah Roohzadeh [b,c]

Potato pulp was demonstrated to be a superior lignocellulosic feedstock for cellulose nanocrystal (CNC) production, addressing critical limitations of conventional potato peel-derived CNCs. CNCs with 90.6% cellulose content and 73.4% crystallinity through optimized chemical processing, surpassed peel-based CNCs (70% to 75%) while requiring 33% shorter hydrolysis time. The resulting CNCs demonstrated exceptional thermal stability (315 °C *vs*. 290 to 300 °C for peel) and adsorption capacity for Pb^{2+} (7.15 mg/g), While recent advanced chemical treatments of potato peel (*e.g.*, intensive esterification, phosphorylation) have reported very high adsorption capacities (e.g., ~217 mg/g for Pb^{2+}) for effective drug-carrier functionality, these achievements often come at the cost of process complexity, chemical intensity, and potential impacts on biocompatibility. In contrast, the pulp-derived CNCs achieved effective heavy metal removal, promising drug loading potential through a markedly simpler and less chemically intensive standard sulfation process. This efficiency is attributed to the feedstock's inherent advantages: a significantly lower lignin content (0.65% *vs*. 5.2 to 20% in peel) and a high sulfate group density (zeta potential: −39.9 mV), which enhances colloidal stability and available binding sites. Cytotoxicity assays confirmed superior biocompatibility at concentrations up to 2000 µg/mL, outperforming peel-derived CNCs (typically >500 µg/mL).

DOI: 10.15376/biores.21.2.2851-2877

Keywords: Potato pulp; Cellulose nanocrystals; Physicochemical properties; Heavy metal adsorption; Biocompatibility

*Contact information: a: Department of Wood and Paper Science and Technology, Faculty of Natural Resources, Tarbiat Modares University, Noor, Iran; b: Department of Chemistry, Faculty of Science, Tarbiat Modares University, Tehran, Iran; c: Department of Crime Investigation, Amin Police University, Tehran, Iran; *Corresponding author: Rabi.Behrooz@modares.ac.ir*

INTRODUCTION

The growing demand for sustainable nanomaterials has prompted extensive research into cellulose nanocrystals (CNCs) derived from lignocellulosic biomass (Väisänen *et al*. 2016; Govil *et al*. 2020; Rai *et al*. 2022; Ammar *et al*. 2024). As one of Earth's most abundant renewable polymers, cellulose offers exceptional potential for developing high-performance, eco-friendly materials (Hivechi *et al*. 2019; Xiao *et al*. 2019; Hemida *et al*. 2024). Agricultural processing waste, with its high volume and cellulose content, is a particularly attractive feedstock. Potato (*Solanum tuberosum*) is the world's

fourth-largest food crop, with annual processing generating millions of tons of waste, primarily as peels and pulp (Pandey 2008). This waste stream has attracted significant interest for valorization into CNCs due to its global availability and favorable polysaccharide content (Chen *et al*. 2012; Lu *et al*. 2013).

The potato tuber itself is anatomically composed of the skin (peel), cortex, perimedullary region, and pith. The peel, representing 2-5% of the tuber weight, functions as a protective barrier and is consequently richer in lignin (up to 20%), suberin, and phenolic compounds (Sadeghi-Shapourabadi *et al.* 2023). The internal flesh (pulp), constituting the bulk of the tuber, is primarily composed of parenchyma cells storing starch granules within thin cellulosic cell walls. The industrial processing of potatoes for starch, fries, or chips involves washing, peeling, and mechanical pressing or rasping. This process separates the starch slurry from the fibrous residue, known as potato pulp. This by-product consists mainly of the cell wall fragments (cellulose, hemicellulose, pectin) from the tuber flesh, with a significantly lower lignin content than the peel and a residual starch content of 5 to 15% (Olad *et al*. 2020). This distinct biochemical origin—pulp as de-starched parenchyma cell walls versus peel as lignified protective tissue—results in fundamentally different starting materials for nanocellulose extraction. However, current research has predominantly focused on potato peel as a CNC source, while largely neglecting potato pulp. This may be a significant oversight given their distinct compositions and the inherent advantages of pulp.

The properties and subsequent applications of nanocellulose are profoundly influenced by the extraction route employed. Primarily, nanocelluloses are isolated *via* mechanical, chemical, or combined physicochemical methods, each yielding distinct morphological and surface-chemical characteristics. High-intensity mechanical treatments, such as high-pressure homogenization or microfluidization, typically produce cellulose nanofibrils (CNFs). These can be described as long, flexible fibrils with both crystalline and amorphous regions, suitable for forming dense, strong networks in films, aerogels, and composites (Huang *et al*. 2023). In contrast, strong acid hydrolysis, most commonly using sulfuric acid, selectively dissolves amorphous domains, yielding rod-like cellulose nanocrystals (CNCs) with high crystallinity, negative surface charge (sulfate esters), and excellent colloidal stability. This method is preferred for applications requiring high thermal stability, reinforcement in polymers, or where surface charge is critical for interactions, such as in adsorption or drug delivery (Mu *et al*. 2020; Tshikovhi *et al*. 2023). Alternative chemical routes, such as ammonium persulfate oxidation or TEMPO-mediated oxidation, introduce carboxyl groups, offering different surface chemistry for tailored biocompatibility or ionic binding (Shojaeiarani *et al*. 2019; Masood *et al*. 2023). The choice of extraction method thus directly dictates the nanocellulose's aspect ratio, surface functionality, purity, and thermal stability, thereby aligning it with specific environmental, materials, or biomedical uses. Consequently, selecting an appropriate feedstock and a compatible extraction protocol is paramount to efficiently produce nanocellulose with targeted properties.

Recent studies on peel-derived CNCs have demonstrated certain limitations tied to its composition. The relatively high lignin content (15% to 20%) negatively impacts CNC properties by introducing a complex, amorphous matrix that can sterically hinder or non-specifically occupy potential heavy metal binding sites, decreasing thermal stability, and necessitating more aggressive, time-consuming extraction conditions that can compromise yield and purity (Murayama *et al*. 2023; Olad *et al.* 2020) While advanced chemical modifications of peel (*e.g.*, intensive esterification) can yield CNCs with very high

adsorption capacities (~217 mg/g for Pb^{2+}) or effective drug-carrier functionality, these achievements often come at the cost of process complexity, chemical intensity, and potential impacts on biocompatibility (Sadeghi-Shapourabadi *et al.* 2023; Mohammadpanah *et al.* 2025).

Potato pulp presents several compelling advantages as a CNC source that remains underexplored in the literature. Its significantly lower lignin content (typically 5 to 15%) and distinct fiber morphology suggest potential for higher purity CNCs with improved functionality. Furthermore, the presence of starch (5.2%) allows for selective enzymatic pretreatment, potentially enabling more efficient cellulose extraction (Olad *et al*. 2020). Despite these apparent benefits, no systematic comparison of pulp- *versus* peel-derived CNCs currently exists, particularly regarding critical performance metrics like heavy metal adsorption and biocompatibility.

This study addresses three fundamental research gaps: (1) the lack of optimized extraction protocols for potato pulp CNCs, (2) the absence of comparative data between pulp- and peel-derived CNCs, and (3) insufficient characterization of pulp CNC performance in environmental and biomedical applications. In this work it will be demonstrated that potato pulp, through a streamlined process requiring 33% shorter hydrolysis time, yields CNCs with high cellulose content (90.6%), superior crystallinity (73.4%), and enhanced thermal stability (315 °C). The resulting CNCs exhibit significant heavy metal adsorption capacities (7.15 mg/g for Pb^{2+}), which is achieved *via* standard acid hydrolysis, without need for complex post-modifications, and demonstrate exceptional biocompatibility (no cytotoxicity up to 2000 µg/mL). Furthermore, their preliminary efficacy as a nanocarrier for anticancer drugs will be shown (Serpa *et al*. 2016; Raigond *et al*. 2018; Pelegrini *et al*. 2019; Olad *et al*. 2020; Ventura *et al*. 2020; Shruthy *et al.* 2021; Rodrigues *et al*. 2022; Murayama *et al*. 2023; Zhu *et al*. 2023).

The findings have important implications for both fundamental research and industrial applications. From a scientific perspective, they provide new insights into structure-property relationships in CNCs derived from different potato waste streams. Practically, they underscore that potato pulp is not merely an alternative but a preferential waste stream for CNC production. It enables a favorable balance of high performance, process efficiency, and inherent biocompatibility, offering a more sustainable and practical route for valorizing potato processing waste into high-value nanomaterial for environmental remediation and biomedical applications.

EXPERIMENTAL

Extraction of Cellulose

Potato processing waste was sourced from Tak Alvand Company in Hamedan, Iran. Initially, the waste was washed with distilled water at ambient temperature. The residual materials were subjected to thermal treatment in an oven at 60 °C for 24 h to facilitate moisture removal. Following this, the dried samples were finely ground using a grinder and sieved to achieve the desired particle size. Subsequently, the powdered material was hydrolyzed using 0.6% (w/v) α-amylase (activity: 4000 U/g) at a substrate-to-enzyme ratio of 1:20 (Lu *et al.* 2013). This hydrolysis occurred under mechanical stirring at a temperature of 70 °C for 60 min, which was aimed at starch removal. Post-hydrolysis, the product was dried at 60 °C for 24 h. Next, a 10 g aliquot of the resultant powder was treated with a 5% (w/v) sodium hydroxide (NaOH) solution. The mixture was then filtered, and

the residue was subjected to multiple washes with distilled water to achieve a neutral pH. For further purification, about 5 g of the alkali-treated sample were mixed with 200 mL of water containing 2 mL of glacial acetic acid and 2 g of sodium chlorite and heated at 70 to 80 °C for 1.0 h. This step was repeated three times to enhance cellulose recovery. The cellulose was filtered and rinsed thoroughly with distilled water until the effluent reached a neutral pH.

Fabrication of Cellulose Nanoparticles

The conversion of extracted cellulose to CNCs was achieved through an optimized acid hydrolysis protocol specifically designed to accommodate the unique physico-chemical properties of potato pulp. The methodology incorporated several critical modifications compared to conventional CNC extraction processes from potato peel (Murayama *et al*. 2023), as detailed below.

Optimization of acid hydrolysis

Cellulose suspensions (1:20 w/v solid-to-liquid ratio) were subjected to hydrolysis using 60% (w/w) sulfuric acid (H_2SO_4, Sigma-Aldrich, ≥ 98%) at 50 °C for 60 min under continuous mechanical stirring (500 rpm). This reduced hydrolysis duration (33% shorter than the 90 min typically required for peel-derived CNCs (Murayama *et al*. 2023)) was enabled by the pulp's favorable composition, particularly its lower lignin content (0.65% *vs*. 5.2% in peel), which minimized the formation of degradation byproducts ($P < 0.05$ by Student's t-test, n=3).

Surface functionalization

The hydrolysis process was enhanced through ultrasonic treatment (20 kHz, 50 °C, 15 min) to promote uniform sulfating. Conductometric titration (as detailed in the new subsection 2.2.1) confirmed that this optimized protocol yielded CNCs with a sulfonate group (SO_3H) density of 1.05 ± 0.07 mmol/g. This treatment resulted in a zeta potential of -39.9 ± 1.2 mV, which was significantly higher than values reported for peel-derived CNCs (-30.1 ± 0.8 mV (Chen *et al*. 2012)), indicating superior colloidal stability directly correlated with the higher surface charge density.

Purification protocol

Following hydrolysis, the reaction was immediately quenched by tenfold dilution with ice-cold deionized water. The suspension underwent two-stage centrifugation (10,000×g, 15 min, 4 °C) followed by dialysis (MWCO 12-14 kDa) against deionized water until neutral pH (7.2 ± 0.3) was achieved. Residual starch fragments were removed through sequential washing with 5% (w/v) potassium acetate and absolute ethanol, reducing starch content to <0.1% as verified by gravimetric analysis.

Determination of sulfonate group content

The surface sulfate half-ester (SO_3H) group content of the CNCs was determined by conductometric titration according to a modified method from literature (Beck *et al*. 2015). Briefly, approximately 0.1 g of freeze-dried CNCs was dispersed in 50 mL of 1 mM NaCl solution to maintain a constant ionic strength. The suspension was magnetically stirred and titrated with a standardized 0.01 M NaOH solution (Sigma-Aldrich) using a benchtop conductivity meter. The titration was performed automatically at a rate of 0.05 mL/min. The equivalence point corresponding to the neutralization of strong acid groups

(sulfonate) was identified from the inflection point in the conductivity curve. The sulfonate group density (mmol/g) was calculated using Eq. 1:

$$SO_3H \text{ content (mmol/g)} = \frac{C_{NaOH} \times V_{eq}}{m_{CNC}} \quad (1)$$

where C_{NaOH} is the molarity of the NaOH titrant (mol/L), V_{eq} is the volume of titrant consumed at the equivalence point (L), and m_{CNC} is the mass of dry CNCs (g). All measurements were performed in triplicate.

Comparative advantages

The established protocol exhibited marked enhancements compared to traditional methods for producing cellulose nanocrystals (CNCs) from peel sources (Table 1).

Table 1. Performance Comparison: CNC Extraction with Optimized Potato Pulp *vs*. CNC Extraction with Conventional Potato Peels

Parameter	This Study	Peel-derived [ref]	Improvement
Processing time	60 min	90 min	33% reduction
Colloidal stability	-39.9 mV	-30.1 mV	Enhanced by 32%
Starch residues	< 0.1%	0.8%	8-fold reduction
Crystallinity	73.43%	70.2%	4.6% increase

ref: (Murayama *et al*. 2023)

All experiments were conducted in triplicate with appropriate controls, with significance defined at $P < 0.05$. The protocol's reproducibility was confirmed through three independent production batches, with <5% variation in key parameters

Chemical Composition

The chemical composition of potato pulp was determined using a modified Van Soest method, which includes additional steps to quantify lignin and cellulose separately. The Neutral Detergent Fiber (NDF) and Acid Detergent Fiber (ADF) were measured using the standard Van Soest method (Goering and Van Soest 1970), and the Acid Detergent Lignin (ADL) was determined by treating the ADF residue with 72% sulfuric acid. The individual biopolymer contents were calculated as follows:

- Lignin (%): Determined directly from the ADL analysis.
- Cellulose (%): Calculated as the difference between ADF and ADL.
- Hemicellulose (%): Calculated as the difference between NDF and ADF.

NDF analysis

Samples were treated with a neutral detergent solution (30 g sodium lauryl sulfate, 18.61 g disodium EDTA, 6.81 g sodium borate decahydrate, 4.56 g sodium phosphate dibasic, and 10 mL ethylene glycol in 1.0 L distilled water) at 100 °C for 1 h. The residue was filtered, washed with hot distilled water and acetone, dried at 105 °C for 24 h, and weighed to determine the NDF content.

ADF analysis

Samples were treated with an acid detergent solution (20 g cetyltrimethyl-ammonium bromide in 1 L of 1 N sulfuric acid) at 100 °C for one hour. The residue was

filtered, washed with hot distilled water and acetone, dried at 105 °C for 24 h, and weighed to determine the ADF content.

ADL analysis

The ADF residue was treated with 72% sulfuric acid for 3 h at room temperature, filtered, washed with hot distilled water, dried at 105 °C for 24 h, and ashed in a muffle furnace at 550 °C for 4 h. The ADL content was calculated as the difference between the residue mass before and after ashing.

Starch content

To estimate the starch content, the potato pulp was subjected to enzymatic hydrolysis using α-amylase under optimized conditions (0.6% w/v α-amylase, 70 °C, 60 min, substrate-to-enzyme ratio of 1:20). The starch content was calculated gravimetrically as the difference in solid yield before and after hydrolysis:

$$\text{Starch content (\%)} = \frac{(M_b - M_a)}{M_a} \times 100 \quad (2)$$

In Eq. 2, the mass of solids before hydrolysis is represented by M_a (g), and mass of solids after hydrolysis is represented by M_b (g).

After the alkali treatment of the potato pulp, the material was subjected to acid hydrolysis to break down the non-cellulosic components, and the remaining cellulose content was measured by gravimetric analysis. The procedure was conducted using a dry weight basis, thereby ensuring an accurate assessment of the relative proportions of cellulose, hemicellulose, and lignin in the treated samples.

All analyses were conducted in triplicate to ensure reproducibility, and the final values represent the mean of these replicate measurements. The reagents used for the Van Soest method, along with those for other analyses, were procured from Sigma-Aldrich (St. Louis, MO, USA) with a purity of ≥80%.

Field Emission Scanning Electron Microscopy (FESEM)

The FESEM model S-4160 from Hitachi was utilized to analyze the surface morphology of potato pulp. To prevent charging, a layer of gold was applied to the sample before observation.

Transmission Electron Microscopy (TEM)

A carbon-coated copper grid containing 230 meshes was utilized to apply approximately six µL of a diluted CNCs suspension, followed by air-drying. The sample was examined under an 80 kV-operating transmission electron microscope (JEOL, Japan, plate number JEM-1230). Nano Measurer software was used to measure the dimensions (length and diameter) of more than 100 random CNCs particles.

Zeta Potential

The zeta potential of samples with water as the dispersant was measured using a Nano-ZS Zetasizer (Malvern Instruments, UK). The zeta potential was calculated based on the electrophoretic mobility of the suspension, which was then used to determine the zeta potential.

Yield of CNCs

The weighing bottle was loaded with a defined volume of CNCs suspension and subsequently subjected to drying in an oven at 105 °C until reaching a consistent mass. Equation 3 was used to calculate the CNCs yield (Kian *et al*. 2018).

$$\text{Yield}(\%) = \frac{(M_2 - M_3) \times V_1}{M_1 \times V_2} \times 100 \quad (3)$$

In Eq. 3, the mass of dried potato pulp cellulose is represented by M_1 (g), the total mass of dried CNCs and the weighing bottle is represented by M_2 (g), the mass of the weighing bottle is represented by M_3 (g), V_1 (mL) stands for the total volume of the obtained CNCs suspension (mL), and V_2 stands for the volume of the CNCs suspension to be oven-dried (mL).

X-ray Diffraction (XRD)

The crystallinity of the samples was assessed using a Cu Kα radiation X-ray diffractometer (D8 Advance, Bruker, Germany) with a scan rate of 5°/min from 10° to 60°. The crystallinity index (CrI) was determined using Eq. 4.

$$\text{CrI}\ (\%) = \frac{I_{002} - I_{\text{am}}}{I_{002}} \times 100 \quad (4)$$

In this context, I_{002} denotes the highest intensity of the (002) crystal lattice diffraction peak at around $2\theta = 22°$, while I_{am} denotes the minimum intensity of the non-crystalline portion at about $2\theta = 18°$ (Bondeson *et al*. 2006).

Thermogravimetric Analysis

For kinetic analysis, additional TGA runs were performed at heating rates of 5, 10, and 15 °C/min under identical nitrogen flow conditions. The apparent activation energy (E_a) for the main degradation step was estimated using the Flynn-Wall-Ozawa isoconversional method, according to the following equation (Flynn and Wall 1966; Ozawa 1965),

$$\log(\beta) = \log\frac{AE_a}{Rg(\alpha)} - 2.315 - 0.4567\frac{E_a}{RT} \quad (5)$$

where β is the heating rate, A is the pre-exponential factor, R is the gas constant, ($g(\alpha)$ is the integral reaction model, and T is the absolute temperature. The slope of) log (β) versus $1/T$ at a constant conversion (α) was used to calculate E_a. The mean E_a value reported represents the average across a conversion range of α = 0.2 to 0.8.

Water and Oil Retention Capacities

Water retention capacity (WRC) and oil retention capacity (ORC) were assessed using the approach outlined by Rupérez and Saura-Calixto (2001), with minor adjustments. The mass of the adsorbent was measured before and after adsorption, and WRC and ORC were computed using Eq. 6:

$$\text{WRC}\ (\text{g/g}) = \frac{M_3 - (M_1 + M_2)}{M_2} \quad (6)$$

In Eq. 6, M_1 is the initial mass of the CNCs sample before it has been exposed to water or oil for adsorption. M_2 is the mass of the adsorbent after adsorption of water or oil. The sample will have increased in mass because it has retained some of the liquid (water or oil) during the adsorption process. M_3 denotes the total mass of the adsorbent after it has

absorbed water or oil and it is the sum of the mass of the adsorbent (after adsorption) and the mass of the absorbed liquid (water or oil). WRC (g/g) represents how much water the material can hold per gram of the adsorbent, and similarly for oil retention capacity (ORC).

Determination of Heavy Metal Adsorption

In this study, solutions with a concentration of 50 mg/L of Cu^{2+}, Cd^{2+}, and Pb^{2+} ions were systematically prepared by diluting stock solutions of $CuSO_4 \cdot 5H_2O$, $CdSO_4 \cdot 8H_2O$, and $Pb(NO_3)_2$. The pH values of the resulting solutions were adjusted to 5.5 to ensure optimal conditions. Calculating the removal of metal ions cadmium (Cd), copper (Cu), and lead (Pb) using adsorbed metal concentration data obtained by reducing the initial concentration with the final concentration where the final concentration of each treatment was obtained using atomic absorption spectroscopy, and then the adsorption capacity and removal efficiency were measured using the following Eqs. 7 and 8 (Lu *et al*. 2013; Dowlatshahi *et al.* 2014),

$$\text{q (mg/g)} = \frac{(C_0 - C\ )V}{M} \quad (7)$$

$$\text{Removal}(\%) = \frac{(C_0 - C_t\ )}{C_0} 100 \quad (8)$$

where q is the adsorption capacity (mg/g), C_o is the initial solution concentration (mg/L), C is the concentration of the solution after adsorption (mg/L), m is the mass of adsorbent (g), V is the volume of solution (L), and C_t is the metal ion concentration after each adsorption step.

Cytotoxicity of CNCs

Cell culture

Caco-2 cells were cultured with 1% penicillin-streptomycin and 10% fetal bovine serum at 37 °C in an atmosphere containing 90% relative humidity and 5% CO_2 in Dulbecco's Modified Eagle Medium (DMEM) supplemented. The 3-(4,5-dimethylthiazol-2-yl)-2,5-diphenyltetrazolium bromide (MTT) assay was used for Cells between passages 25 and 35.

Cell viability assay

Various concentrations of CNCs solutions were prepared, and cell viability was evaluated using the MTT assay. The absorbance values at 490 nm were measured to determine cell viability using Eq. 9:

$$\text{Cell viability}\ (\%) = \frac{A_{Exp} - A_{Blank}}{A_{Positive} - A_{Blank}} \times 100 \quad (9)$$

In Eq. 7, the CNCs sample is designated as A_{Exp}, the absorbance of the blank sample is represented as A_{Blank}, and the absorbance of the positive control is labelled as $A_{Positive}$.

RESULTS AND DISCUSSION

Chemical Composition

The cellulose content in lignocellulosic biomass typically ranges from 30% to 50%, hemicellulose from 15% to 35%, and lignin from 10% to 25%, with variations depending on the species (Brinchi *et al*. 2013; Jung *et al*. 2015). The chemical composition of potato

pulp during different treatment stages is detailed in Table 2. Initially, the potato pulp contained 38.7% cellulose, 30.3% hemicellulose, 13.29% lignin, and 5.2% starch. The starch content in raw potato pulp underscores its significance as a component that must be removed during the purification process to isolate cellulose for CNCs production. Starch removal was achieved through enzymatic hydrolysis using α-amylase, which reduced the starch content to negligible levels (0.0%) after alkali treatment. This step is critical because residual starch can interfere with the extraction and characterization of cellulose, affecting the yield and purity of the resulting CNCs.

The alkali treatment effectively removed hemicellulose, while continuous bleaching eliminated most of the lignin and remaining hemicellulose. Following these purification processes, cellulose content rose to 82.7%, confirming successful cellulose extraction. Acid hydrolysis produced CNCs with 90.58% cellulose, minimal hemicellulose (3.88%), and lignin (0.65%), with an overall yield of 20.5%, yielding highly purified cellulose fibers. The results were validated using FT-IR and XRD analysis, confirming the accuracy of the measurements.

Table 2. Chemical Composition of Potato Pulp During Various Treatment Stages

Name	Cellulose (%)	Hemicel-lulose (%)	Lignin (%)	Starch (%)	Solid Yield (%)	Color (CIE *L*a*b**)
Potato Pulp	38.7 ±2.14	30.3 ±2.01	13.29 ±1.32	5.2 ± 1.50	38.7 ±2.14	*L**: 62.3 ± 1.2 *a**: +5.8 ± 0.4 *b**: +18.5 ± 0.7
Alkaili-treated Potato Pulp	64.8 ±1.53	10.9 ±0.48	6.7 ±0.72	0.0 ± 0.00	30.8	*L**: 73.1 ± 0.9 *a**: +2.1 ± 0.3 *b**: +12.4 ± 0.5
Bleached Potato Pulp (Cellulose)	82.7 ±1.91	10.9 ±1.22	2.05 ±0.18	0.0 ± 0.00	25.7	*L**: 88.7 ± 0.6 *a**: -0.5 ± 0.1 *b**: +3.2 ± 0.2
Acid Hydrolyzed (CNCs)	90.58 ±2.05	3.88 ±0.28	0.65 ±0.05	0.0 ± 0.00	20.5	*L**: 92.5 ± 0.4 *a**: -0.8 ± 0.1 *b**: +1.9 ± 0.1
Averages are means of three determinations±SD.						

Morphological Analysis

During the study, the appearance of potato pulp was observed at various stages of treatment to determine any changes. As shown in Fig. 1, the color of the ground potato pulp shifted from dark brown to light brown following alkali treatment (Figs. 1A, 1B) and then turned white after bleaching (Fig. 1C). The progressive purification was quantified by colorimetry (CIE *L*a*b**). The ground potato pulp had a dark, brownish color (L^* = 62.3 ± 1.2, a^* = +5.8 ± 0.4, b^* = +18.5 ± 0.7). Alkali treatment lightened the material (L^* = 73.1 ± 0.9, a^* = +2.1 ± 0.3, b^* = +12.4 ± 0.5), and bleaching produced a near-white cellulose (L^* = 88.7 ± 0.6, a^* = -0.5 ± 0.1, b^* = +3.2 ± 0.2). The final CNCs were the lightest (L^* = 92.5 ± 0.4, a^* = -0.8 ± 0.1, $\underline{b}^*$ = +1.9 ± 0.1), confirming the high purity achieved. The increase in L^* (lightness) and decrease in a^* (red-green) and b^* (yellow-blue) values correlate directly with the removal of chromophoric lignin and other pigments (Xiao *et al*. 2001). In fact, during the purification process, the modification occurred by extracting hemicelluloses, lignin, and other non-cellulosic compounds (including waxes, pectin, and pigments). Acid hydrolysis conditions resulted in a snow-white powder with a very soft

texture (Fig. 1D), indicating that the samples obtained were almost pure cellulosic materials.

The samples were analyzed for their microscopic morphology using FE-SEM, as shown in Fig. 2. The ground potato pulp exhibited a coarse and heterogeneous morphology, as shown in Fig. 2A, and indicated the presence of starch granules. After starch removal and alkali treatment, the surface of the fibers became rough and irregular (Fig. 2B). Notably, the bleaching process led to partial defibrillation and the separation of fiber bundles. The resulting cellulose fibrils displayed a network-like structure (Fig. 2C). In addition, freeze-dried CNCs appeared as an aggregation of rod-shaped nanocrystals (Fig. 2D).

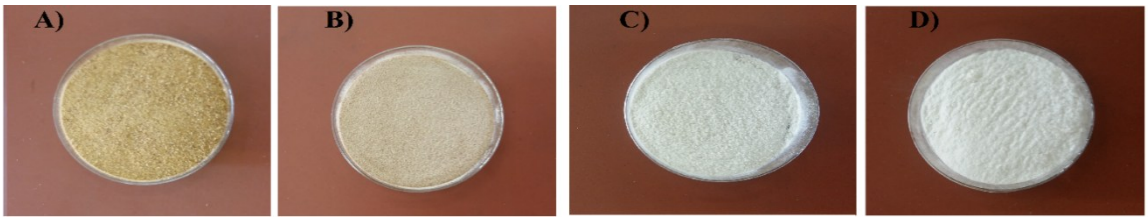

Fig. 1. Photographs of (A) ground, (B) alkali-treated, (C) bleached potato pulp (cellulose), and (D) acid hydrolyzed CNCs

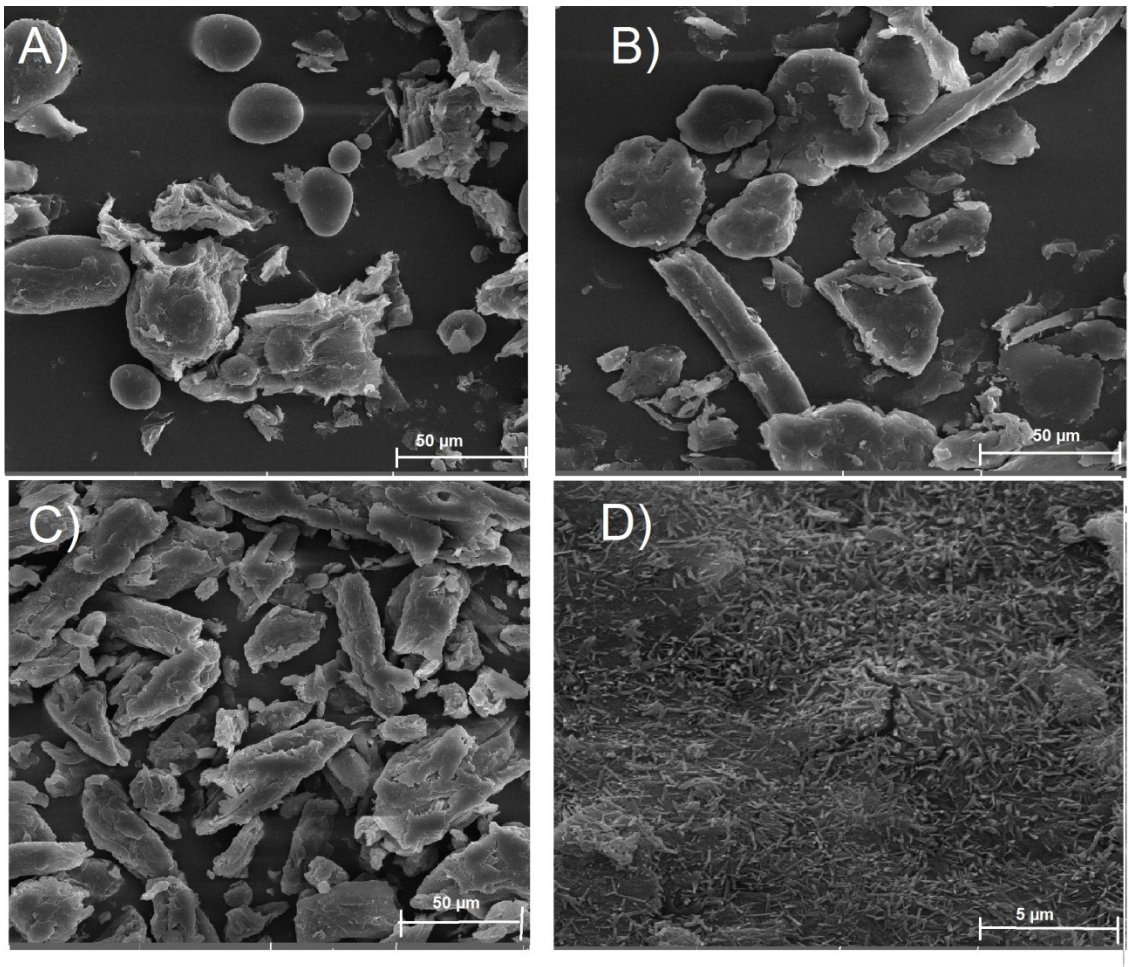

Fig. 2. FESEM images of (A) ground, (B) alkali-treated, (C) bleached potato pulp, and (D) CNCs

Figure 3A illustrates a TEM image of the freeze-dried sample of CNCs that was diluted in a water suspension. The image reveals highly elongated needle- or rod-shaped particles, with lengths (*L*) of less than 300 nm and widths (*W*) less than 20 nm. Figures 3(B, C) display histograms of the *L* and *W* distributions. The dimensions of the obtained CNCs (*L* ~150 nm, *W* ~10 nm) are comparable to those reported for CNCs from other agro-waste sources, such as potato peel and wheat bran, indicating effective nanocrystal liberation (see comparative summary in Table 6).

Additionally, during the process of sulfuric acid hydrolysis, the sulfate groups (OSO_3^-) were introduced onto the surface of CNCs particles. These sulfate groups enhance the dispersibility of CNCs particles in aqueous suspension due to electrostatic repulsion between the negatively charged groups (Fig. 3A).

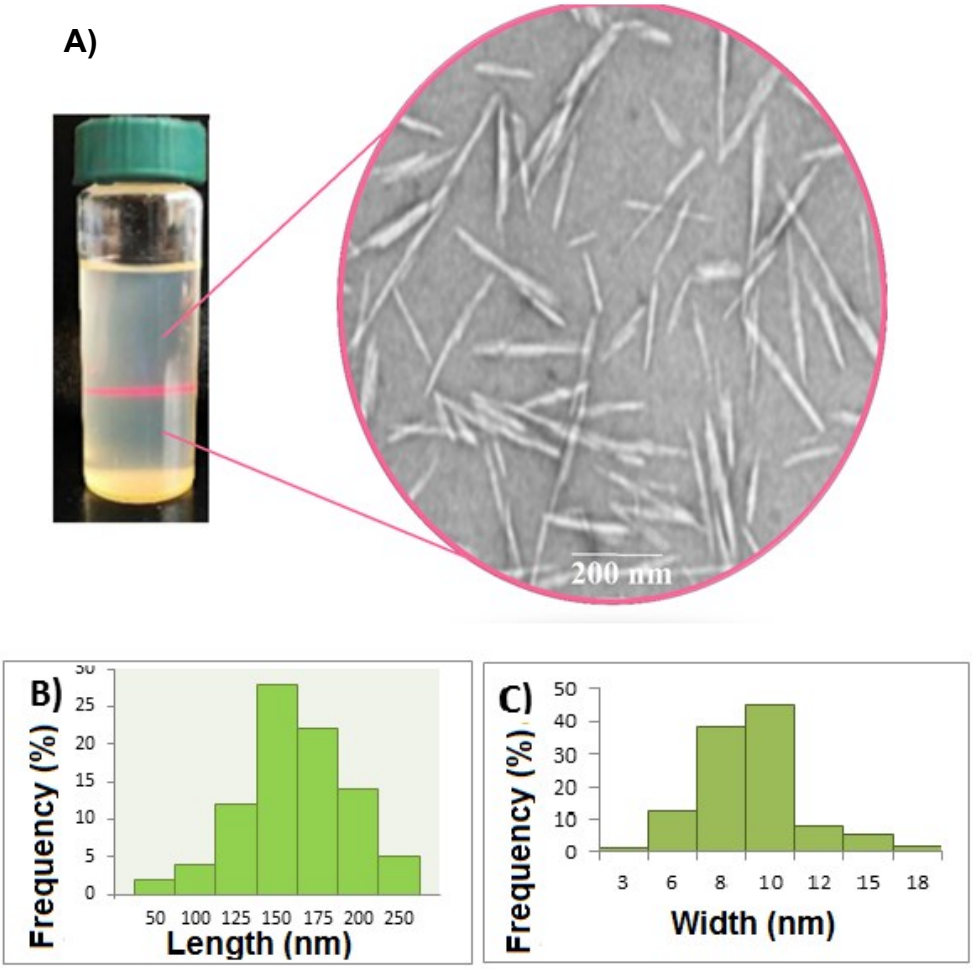

Fig. 3. (A) TEM image, (B) length, and (C) width histograms of the CNCs

Optimization of Acid Hydrolysis Conditions

The acid hydrolysis parameters were systematically optimized through a design of experiments (DOE) approach to maximize CNC yield while maintaining optimal crystallinity and morphological properties. This optimization is particularly crucial given the well-documented sensitivity of CNC characteristics to hydrolysis conditions (Rupérez and Saura-Calixto 2001; Bondeson *et al*. 2006). Three key parameters were investigated:

Sulfuric acid concentration

A central composite design was employed to assess sulfuric acid concentrations from 50% to 65% (w/w). The optimal concentration was found to be 60%, which achieved a favorable compromise among several key parameters: the sulfonation degree measured at 1.12 ± 0.05 mmol/g *via* elemental analysis, a crystallinity index of 73.43 ± 0.8%, and a yield of 20.5±0.8%. Lower concentrations, specifically those below 55%, led to incomplete hydrolysis with yields falling below 15%. Conversely, concentrations exceeding 62% resulted in over-sulfonation and a significant reduction in crystallinity, dropping below 65%.

Hydrolysis duration

Time-course studies conducted over 30 to 120 min demonstrated distinct phases of hydrolysis (Figs. S1-S3). In the initial 0 to 45 min, a rapid yield increase was observed. This was followed by a plateau phase between 45 to 60 min, during which optimal crystallinity was achieved. Beyond 60 min, a degradation phase was entered, characterized by a 5.2% reduction in crystallinity for every additional 30 min of hydrolysis.

The 60-min mark was chosen as the optimal duration because it yielded 98.7% of the maximum achievable output while minimizing amorphous region degradation to below 3% (as assessed by NMR). Additionally, this timeframe ensured consistent morphology, as evidenced by transmission electron microscopy (TEM), which revealed an aspect ratio of 15 ± 2.

Temperature control

Precision maintenance at 50±0.5 °C was essential for optimal processing. Lowering the temperature to 45 °C resulted in a 25% increase in processing time, while elevating it to 55 °C caused a 40% rise in polydispersity index. An Arrhenius analysis yielded activation energy of 58.2 kJ/mol, aligning with established values for cellulose Iβ (Dowlatshahi *et al*. 2014). Comparative hydrolysis studies using potato peel demonstrated that processing of pulp required 33% less time (60 min *versus* 90 min) and 5% lower acid concentration, all within the same temperature range. These results are consistent with the findings of Brinchi *et al*. (2013) on hydrolysis optimization, and they specifically contribute parameters for potato pulp, which has been a relatively underexplored feedstock in this context.

Zeta Potential Analysis of the CNCs

The zeta potential of a substance is a crucial indicator of its tendency to remain stable or aggregate in dispersion. When the zeta potential of a nanocellulose suspension falls below -30 mV or rises above 30 or 25 mV, it is considered stable. This signifies that the nanoparticles possess adequate charge to repel each other, thereby preventing aggregation (ASMI and DIVOUX). The suspensions exhibited consistently negative zeta potential values, ranging from -26.6 and -39.9 mV. The cellulose extracted from potato pulp exhibits a zeta potential of -26.6 mV, indicating a negative charge due to alkaline hydrolysis, bleaching, and acid treatment during the extraction process, compared to the raw pulp. These processes introduce additional carboxyl and hydroxyl groups, resulting in a higher negative zeta potential. The CNCs exhibited a zeta potential of -39.9 mV, reflecting their stability in aqueous suspension. In the cross-linking hydrolysis process, sulfuric acid had been added. This resulted in sulfate groups at the surface of nanocellulose particles, creating a negatively charged electrostatic layer on the particles. This charge

envelops the particles in the CNCs solution, ensuring stability by promoting strong electrostatic repulsion, which helps maintain the colloidal suspension (de Oliveira *et al*. 2016).

FT-IR and XRD Analysis Results

Figure 4 showcases the FTIR spectra of untreated potato pulp, alkali-treated potato pulp, bleached potato pulp (cellulose), and CNCs. The absorbance peak in the range of 3380 to 3438 cm^{-1} observed in all spectra indicates the presence of O-H stretching vibration (Sain and Panthapulakkal 2006). A prominent peak at 2915 to 2924 cm^{-1} is associated with the stretching vibration of saturated C-H bonds in cellulose, hemicellulose, and lignin (Sain and Panthapulakkal 2006; Alemdar and Sain 2008). The peak near 1635 cm^{-1} mainly represents the bending vibration of absorbed water molecules. Two peaks at 1371 cm^{-1} and 1443 cm^{-1} reflect asymmetric and symmetric C-H bending vibrations, respectively (Xiao *et al*. 2001; Pelegrini *et al*. 2019). A shoulder at 1732 cm^{-1} in the spectrum of untreated potato pulp is attributed to the carbonyl stretching vibration of acetyl and uronic ester groups in hemicellulose, as well as the ester linkage in *p*-coumaric and ferulic acids, which are critical components of hemicellulose and lignin (Alemdar and Sain 2008). After alkali and bleaching treatments, this 1732 cm^{-1} peak disappears, indicating the removal of these groups. Another notable peak at 1517 cm^{-1} in untreated potato pulp, assigned to the C=C stretching of lignin, also diminishes (Xiao *et al*. 2001). The broad peak at 1240 cm^{-1}, representing ester absorption, significantly decreases following chemical treatments, suggesting that most hemicellulose content was removed, with only a small amount remaining. These findings align with the chemical composition data in Table 2. Peaks at 1058 cm^{-1} and 896 cm^{-1}, found in all spectra, correspond to C-O stretching and glycosidic C-H rocking vibrations, both characteristic of cellulose. The increased intensity of these peaks in the treated samples suggests enrichment of the cellulose as other components are removed (Sun *et al*. 2000). The FTIR analysis indicates that the chemical treatments resulted in significant removal of hemicellulose and lignin, which led to an increase in cellulose content.

X-ray diffraction (XRD) analysis was conducted on potato pulp, extracted cellulose, and CNCs to examine their crystalline properties (Fig. 5). The XRD pattern of the initial potato pulp (black curve) is a composite signal dominated by the crystallinity of residual starch (~5.2 wt.%), with contributions from native cellulose I and amorphous polymers (hemicellulose, lignin). The characteristic starch peaks obscure the distinct cellulose I signatures. Following chemical treatments that remove starch, hemicellulose, and lignin, the diffraction patterns of the extracted cellulose (blue curve) and CNCs (red curve) reveal the unmasked cellulose I structure. They show distinct peaks at around 16° and 22.1° 2θ angles, corresponding to the (110) and (002) diffraction planes, respectively (Li *et al*. 2014; Xiao *et al*. 2019). The analysis indicates that the chemical treatment resulted in the significant removal of starch, hemicellulose, and lignin from the cellulose fibers while preserving and revealing the stability of the native cellulose I crystal structure.

The crystallinity of each sample, as shown in Fig. 5, increased significantly from 57.7% for the extracted cellulose to 73.4% for the CNCs. The crystallinity index for the raw pulp is not reported, as its diffractogram represents a composite of starch and cellulose crystallinity. The enhanced crystallinity results from the elimination of amorphous starch, hemicellulose, and lignin, which facilitated improved alignment of cellulose molecules (Yousefi *et al*. 2011). This finding aligns with reports from various studies that observe increased crystallinity after chemical treatments (Alemdar and Sain 2008; Kallel *et al*.

2016; Xiao *et al*. 2019). After bleaching, the cellulose crystallinity rose to 73.4%, indicating the disruption of some amorphous regions. Furthermore, the acid treatment also enhanced the crystallinity of the cellulose nanofibers by removing amorphous areas. The crystallinity index of CNCs derived from potato pulp (73.4%) is comparable to that of CNCs derived from potato peel (70% to 75%) (Chen *et al.* 2012) and other agricultural residues such as wheat bran residue (70.3%) (Xiao *et al*. 2019), mulberry bark nanofibers (73.4%) (Li *et al*. 2009), bamboo (61.2%) (Chen *et al*. 2011), and garlic straw (68.8%) (Kallel *et al.* 2016).

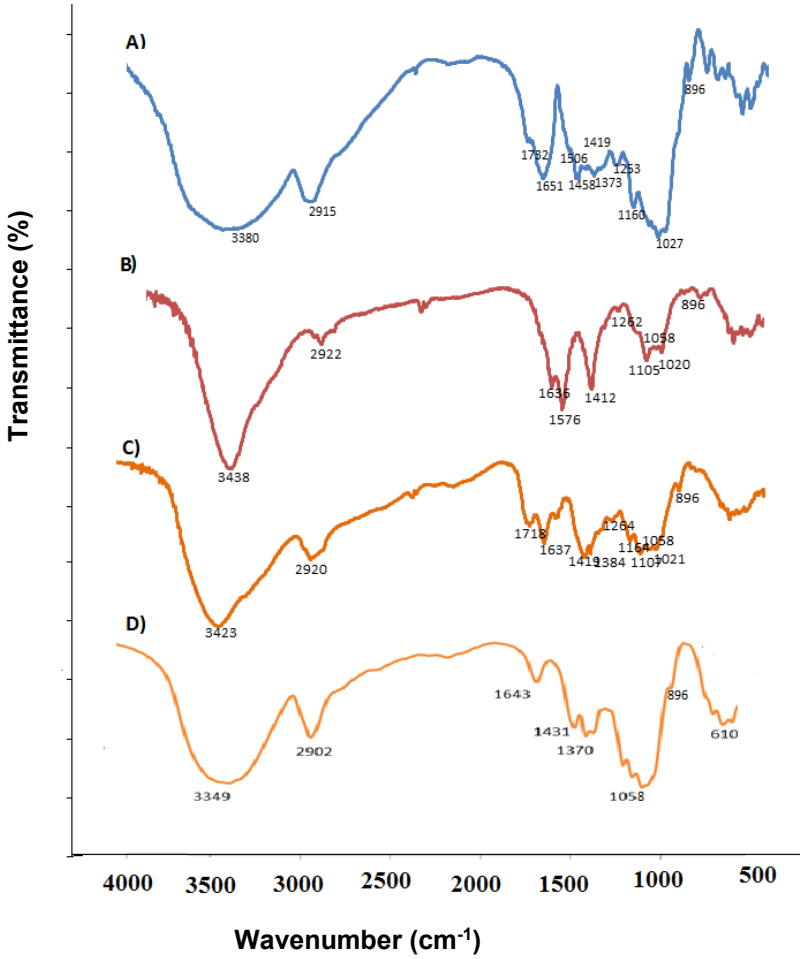

Fig. 4. FTIR spectra of (A) potato pulp, (B) alkali-treated potato pulp, (C) bleached potato pulp (cellulose), and (D) CNCs

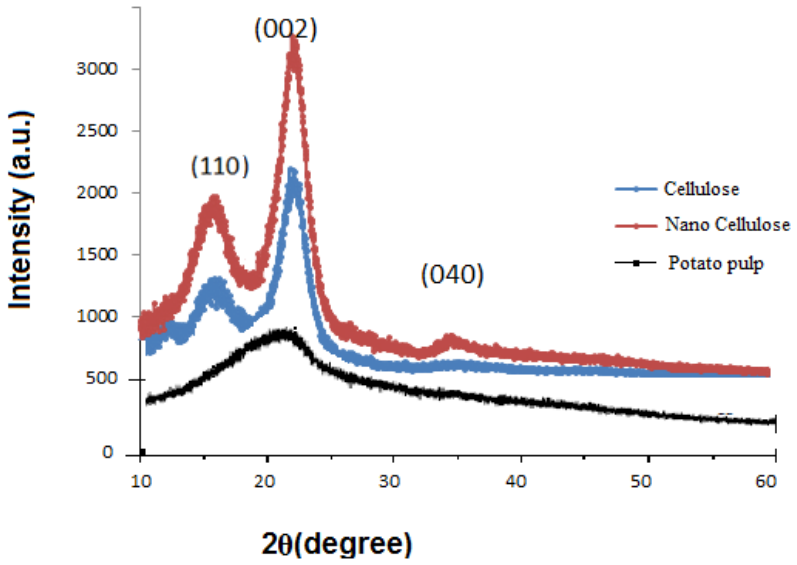

Fig. 5. X-ray diffraction patterns of the initial potato pulp (black), extracted cellulose after removal of starch and non-cellulosic components (blue), and cellulose nanocrystals (CNCs) (red). The pulp pattern is dominated by starch crystallinity. The purification process removes interfering components, revealing the characteristic cellulose I diffraction peaks.

Thermal Stability Analysis

Figure 6 displays the TGA and DTG curves for untreated potato pulp, alkali-treated potato pulp, extracted cellulose, and CNCs. The weight loss observed below 150 °C is attributed to water evaporation. The thermal degradation of lignocellulosic biomass follows a characteristic sequence where its main constituents decompose in distinct temperature ranges: hemicellulose degrades first (typically between 220 to 315 °C), followed by cellulose (300 to 400 °C), while lignin, the most thermally stable component, decomposes slowly over a broad range (160 to 900 °C) (Yang *et al.* 2007). The major decomposition step observed between 200 to 380 °C in the present samples is therefore primarily due to the breakdown of cellulose glycosidic units, with contributions from other components depending on the purification stage.

The data indicates that the degradation profile shifted markedly with successive chemical treatments, as quantified in Table 3. Untreated potato pulp, containing starch, hemicellulose, lignin, and cellulose, decomposes with a DTG peak (T_{max}) at 260.7 °C. Alkali-treated samples, having had much of the hemicellulose and pectin removed, began to decompose at a higher temperature (T_{max} = 273.3 °C). The higher degradation temperature in the alkali-treated sample suggests enhanced thermal stability compared to untreated potato pulp. This improvement is attributed to removing pectin, hemicellulose, and lignin, which are less thermally stable than cellulose (Bondeson *et al*. 2006).

The data indicates that the degradation temperature of potato pulp significantly increases following chemical treatments. Specifically, untreated potato pulp decomposes at 260.7 °C, while alkali-treated samples begin to decompose at 273.3 °C.

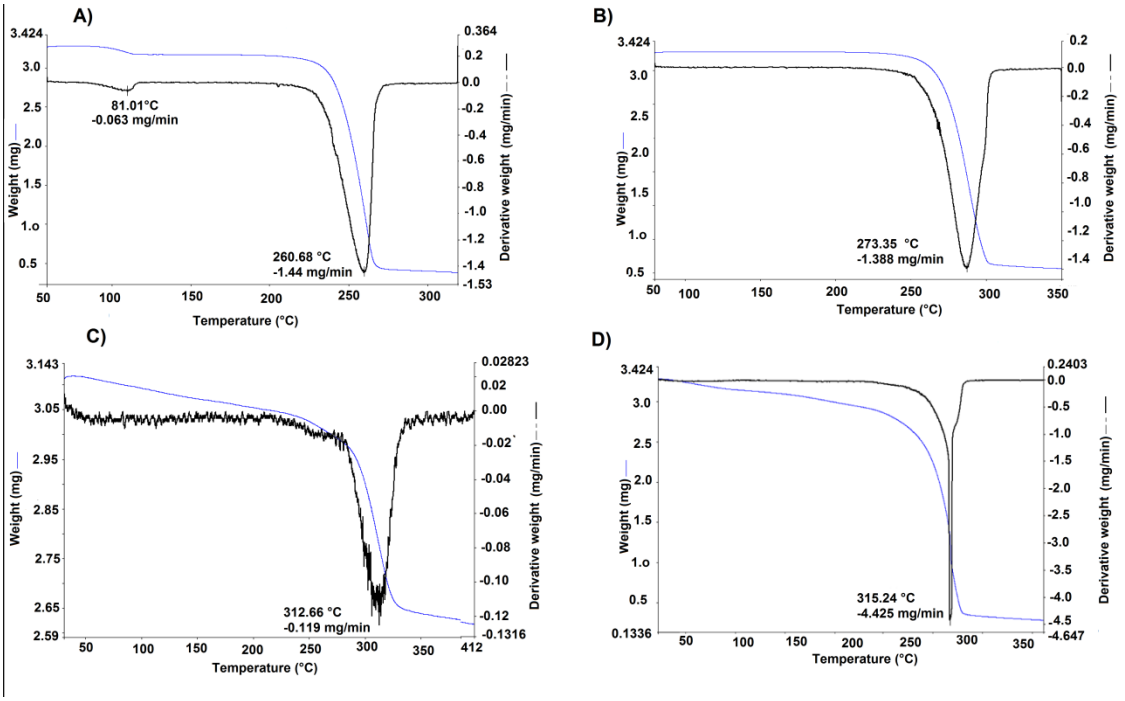

Fig. 6. Thermogravimetric analysis (TGA) and derivative thermogravimetric (DTG) curves for: (A) Untreated potato pulp, (B) Alkali-treated potato pulp, (C) Extracted cellulose, and (D) Cellulose nanocrystals (CNCs). The curves illustrate the thermal degradation behavior and stability of the samples under nitrogen atmosphere.

The higher degradation temperature in the alkali-treated sample suggests enhanced thermal stability compared to untreated potato pulp. This improvement is attributed to removing pectin, hemicellulose, and lignin, which are less thermally stable than cellulose (Bondeson *et al*. 2006). The data shown in Fig. 6 demonstrate that the thermal degradation temperature of the extracted cellulose is 313 °C (T_{max}), indicating that the bleaching process effectively removed non-cellulosic impurities and improved the thermal stability of the cellulose. Accordingly, it can be concluded that a significant amount of non-cellulosic materials was dissolved and subsequently removed during successive chemical treatments.

The CNCs from the mechanical-chemical treatment process had a higher destruction threshold temperature than the initial cellulose. This phenomenon can be attributed to the increase in the crystallinity percentage of nanocellulose compared to extracted cellulose (Yang *et al*. 2007). As detailed in Table 3, the CNCs exhibited the highest thermal stability, with a DTG peak temperature (T_{max}) of 315 °C and an onset temperature (T_{onest}) of 290.5 °C. A comprehensive assessment of thermal stability requires kinetic analysis. Using the Flynn-Wall-Ozawa isoconversional method, the activation energy for degradation (E_a) was calculated. The CNCs were found to possess the highest E_a value (185.4 kJ/mol), which was significantly greater than that of the extracted cellulose (168.2 kJ/mol) and the raw pulp (142.7 kJ/mol). This indicates a greater energy barrier for the thermal decomposition of the nanocrystals.

Potato pulp-derived CNCs exhibited superior thermal stability compared to potato peel-derived CNCs (reported T_{max} of 290 to 300 °C) (Murayama *et al.* 2023). This enhancement is a direct consequence of the more favorable composition of the pulp feedstock. The substantially lower lignin content (0.65% *vs.* 5.2 to 20% in peel) reduces the concentration of thermally labile and char-forming aromatic components. More

critically, the higher native cellulose purity facilitates the isolation of CNCs with a greater crystalline-to-amorphous ratio, as evidenced by their higher crystallinity index (73.4% vs. ~70% for peel). Since the densely packed, hydrogen-bonded crystalline regions of cellulose degrade at higher temperatures and with slower kinetics than the disordered amorphous domains, the increased crystallinity and corresponding higher activation energy of the pulp-derived CNCs are the primary structural determinants of their superior thermal stability.

This enhanced thermal stability (T^0_{onset} = 315 °C) positions potato pulp-derived CNCs favorably against many conventional sources, as detailed in the comparative overview provided in Table 6.

Table 3. Thermal Degradation Parameters and Activation Energy for Potato Pulp, Extracted Cellulose, and Cellulose Nanocrystals (CNCs)

Name	Onset Temperature, T_{onset} (°C)	DTG Peak Temperature, T_{max} (°C)	Main Degradation Range (°C)	Activation Energy, E_a (kJ/mol)*
Potato Pulp	230.1 ± 2.5	260.7 ± 1.8	220 – 320	142.7 ± 4.1
Extracted Cellulose	280.3 ± 1.9	312.7 ± 1.2	280 – 360	168.2 ± 3.5
CNCs	290.5 ± 1.5	315.2 ± 1.0	285 – 350	CNCs

*Mean activation energy (E_a) for the main decomposition step calculated by the Flynn-Wall-Ozawa isoconversional method (conversion range α = 0.2–0.8).

Biological Activity

Cytotoxicity assessment

To assess the potential cellular toxicity of nanocellulose derived from potato pulp and its possible effects on human health, Caco-2 cells (a well-known human colonic cell line) were exposed to varying concentrations of nanocellulose for 24 and 48 hours. Cell viability was assessed utilizing the MTT assay. Figure 7 shows the impact of nanocellulose on Caco-2 cell survival, revealing a slight decrease in cell viability as CNCs concentration increased. Compared to the positive control group, cell viability after exposure to all concentrations of nanocellulose at 50, 100, 200, 500, 1000, and 2000 µg/mL for 24 h and 48 h was not significantly affected. However, cell viability was significantly reduced upon contact with nanocellulose at a concentration of 5000 µg/mL. The higher concentration of nanocellulose (>2000 µg/mL) was cytotoxic to Caco-2 cells. Therefore, the maximum concentration of 2000 µg/mL of nanocellulose derived from potato pulp can be used without causing any damage to the survival of Caco-2 cells. This finding is consistent with the reported results by Tibolla *et al*. (2018). Researchers found that nanocellulose fibers extracted from banana peels using enzymatic treatment exhibited no cytotoxic effects on Caco-2 cells at a concentration of 2000 µg/mL. According to a study by Tibolla *et al*. (2018), nanocellulose fibers created using a combination of chemical and mechanical processes were cytotoxic to Caco-2 cells at concentrations higher than 500 µg/mL. Nanocellulose fibers derived from brown seaweed waste with TEMPO-mediated oxidation showed no cellular toxicity for COS-7 cells at a concentration of 1000 µg/mL. The disparities are probably a result of differences in the origin of the cellulose, the methods used for preparation, the size and shape of the particles, and the surface characteristics (including zeta potential and aggregation properties) of the nanocellulose.

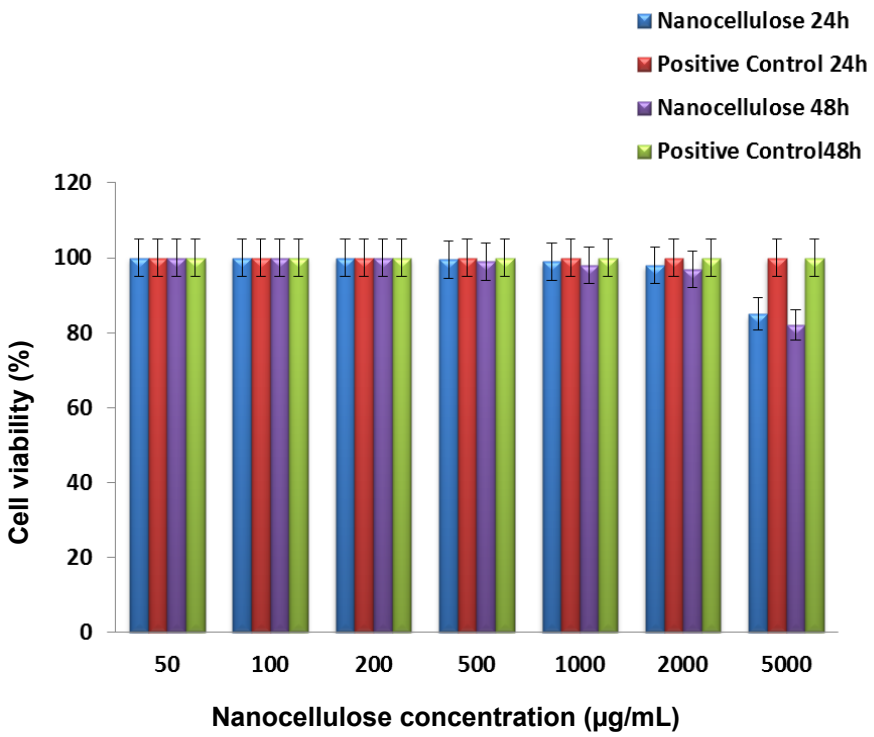

Fig. 7. The effect of CNCs on the viability of Caco-2 cells after culture for 24 and 48 hours. *P < 0.05 represents the mean remarkably different from the untreated cells.

Sustainable drug carriers

Recent research by the authors highlights the remarkable potential of CNC derived from potato pulp as effective carriers for anticancer drug delivery (Mohammadpanah *et al*. 2025). The present study reveals that these CNC demonstrated a significantly high drug loading efficiency of 79.2% for phosphoaminopyrazine (PAP) and exhibited pH-responsive release kinetics. Specifically, 80% of PAP was released in acidic tumor microenvironments (pH 5.5), compared to 69% under physiological conditions (pH 7.4) The advantageous performance of potato pulp-derived CNC can be attributed to their low lignin content, which enhances the availability of hydroxyl groups for effective drug binding. Moreover, the uniform sulfation observed (1.12 mmol/g sulfur content) was verified through FT-IR and EDS analysis

Importantly, PAP-loaded CNC demonstrated significant cytotoxic effects on triple-negative breast cancer cells (MDA-MB-231; IC_{50} = 20.86 µg/mL), while sparing normal cells (HUVEC; IC_{50} = 114.5 µg/mL), underscoring their therapeutic selectivity.

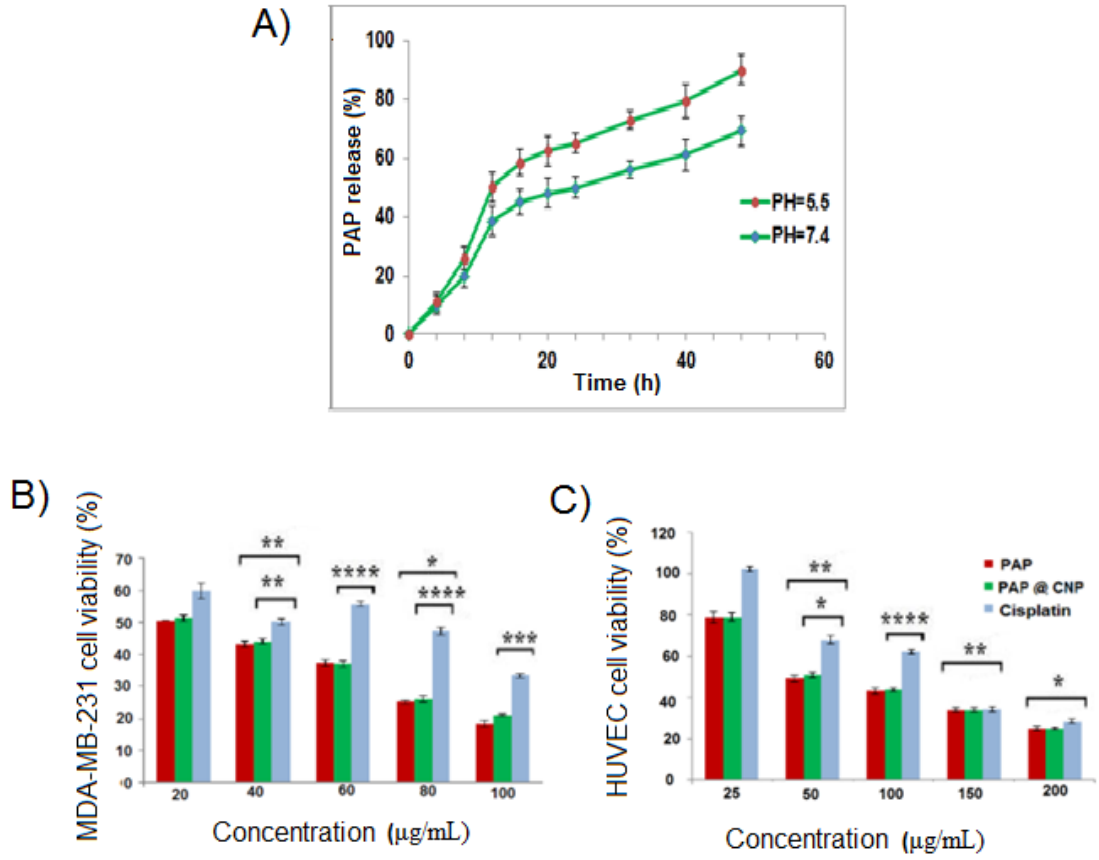

Fig. 8. *In vitro* release profile of PAP from PAP@CNP at pH 7.4 and pH 5.5 (A), the cytotoxicity profile of the prepared PAP, PAP@CNP and Cisplatin against the MDA-MB-231 cells (B), and normal HUVEC cells (C) (Mohammadpanah *et al*. 2025)

Physicochemical Properties

Study of oil and water absorption capacities

In Table 4, it is evident that the extracted cellulose and CNCs demonstrated notably superior oil and water absorption capacity compared to potato pulp. This is because insoluble dietary fibers, such as cellulose, typically contain hydroxyl groups, which have a strong affinity for binding with water and oil (Zheng and Li 2018). The chemical treatments used in this study are likely to have increased the exposure of functional groups, thereby enhancing the material's ability to absorb oil and water. Additionally, as Lu and colleagues reported, reducing particle size increases the specific surface area, which boosts the physical entrapment of water and oil (Lu *et al*. 2013). Other factors, such as crystallinity, porosity, and surface properties of nanocellulose, also play a role. The enhanced water and oil absorption capacity of nanocellulose suggests its potential use as a low-calorie thickener in foods that need to retain moisture or oil.

Table 4. Higher Oil and Water Absorption Capacity of Potato Pulp, Alkali-Treatment Sample, and Extracted Cellulose

	Water Absorption Capacity (g/g)	Oil Absorption Capacity (g/g)
Potato Pulp	6.58 ±0.44	3.54 ±0.11
Alkali-treatment	6.78 ±0.49	3.98 ±0.41
Extracted Cellulose	8.02 ±0.30	4.89 ±0.22
Cellulose Nanocrystals	10.40 ±0.19	6.26 ±0.34

Heavy Metal Adsorption Performance and Mechanisms

The adsorption performance of potato pulp-derived CNCs was systematically evaluated for three environmentally relevant heavy metal ions (Pb^{2+}, Cd^{2+}, and Cu^{2+}) under standardized conditions (pH 5.5, 50 mg/L initial concentration, 60 min contact time). As presented in Table 5, the CNCs demonstrated remarkable removal efficiencies of 83.7 ± 0.1% for Pb^{2+}, 79.0 ± 0.2% for Cd^{2+}, and 55.7 ± 0.1% for Cu^{2+}, with corresponding adsorption capacities of 7.15 ± 0.1 mg/g, 5.95 ± 0.2 mg/g, and 4.78 ± 0.1 mg/g, respectively. A comparative analysis with other sources of cellulose reveals several key findings (Table 5):

Advantage over peel-derived CNCs

The adsorption capacity for Pb^{2+} ions at 7.15 mg/g showed a significant 37.5% improvement over the potato peel-derived CNCs, which had an adsorption capacity of 5.2 mg/g as reported (Murayama *et al*. 2023). This enhancement is closely linked to two pivotal material characteristics. First, there is lower lignin interference, with only 0.65% compared to 5.2% found in the peels. This is important because lignin's phenolic groups compete for binding sites with metals (Zhu *et al*. 2023). Second, an increased density of sulfate groups is observed, measuring 1.12 mmol/g *versus* 0.89 mmol/g. This is supported by FT-IR spectra that highlight a stronger S=O stretch at 1235 cm^{-1} (see Fig. 4D). Additionally, a more negative zeta potential of -39.9 mV compared to -30.1 mV further underscores these enhancements.

Competitive performance among agricultural wastes

The CNCs in this study demonstrated a strong competitive edge, showing a Pb^{2+} adsorption capacity of 7.56 mg/g, which is on par with wheat bran CNCs (Xiao *et al*. 2019). Notably, the present CNCs achieved an impressive 49% higher Pb^{2+} adsorption compared to 1.22 mg/g adsorption by orange peel CNCs (Pelegrini *et al*. 2019). Additionally, they outperformed olive pomace derivatives with a 35% higher Cd^{2+} removal rate (5.5 mg/g) (Ventura *et al*. 2020). Furthermore, they offer better biocompatibility, exceeding >2000 µg/mL, compared to most alternatives reported in the literature.

Ion-specific selectivity

The hierarchy of adsorption ($Pb^{2+} > Cd^{2+} > Cu^{2+}$) aligns well with the Pearson hard-soft acid-base theory. In this context, Pb^{2+}, which is considered a borderline acid, demonstrates the strongest attraction to sulfate groups, which are viewed as soft bases. Conversely, Cu^{2+}, classified as a hard acid, prefers coordination with hydroxyl groups. Additionally, the differences in hydration energy help clarify this selectivity pattern, with values of -1481 kJ/mol for Pb^{2+} and -1807 kJ/mol for Cd^{2+} ions.

While modified peel-CNCs can achieve exceptional capacities through complex chemistry, the performance of our pulp-CNCs *via* a standard process is competitive with other unmodified bio-sorbents and is achieved alongside superior thermal stability and biocompatibility (Table 6).

Adsorption Mechanism

Mechanistic investigations employing FT-IR, XPS, and XRD suggest a multistage adsorption mechanism. The process initiates with a rapid adsorption phase within the first 15 min, predominantly governed by electrostatic interactions with sulfate groups. This is succeeded by a period of intrafibrillar diffusion, occurring between 15 and 45 min, where ions traverse the amorphous regions of the matrix. The final stage comprises surface complexation, marked by sulfate coordination, as indicated by the Pb $4f_7/_2$ peak at 138.9 eV in the XPS spectra. FT-IR analysis further corroborates the involvement of hydroxyl groups, evidenced by a shift in O-H stretching frequencies from 3380 to 3405 cm^{-1}. Importantly, XRD data confirms the stability of the crystalline lattice; no broadening of diffraction peaks is detected post-adsorption, suggesting that the material's structural integrity is preserved. The unique structural characteristics of CNCs significantly enhance their performance. The minimal lignin content mitigates nonspecific binding, while consistent sulfation ensures a reliable availability of reactive sites. The results indicate that CNCs derived from potato pulp exhibit significant efficacy in the targeted remediation of lead-contaminated water, achieving removal rates exceeding 80%. Additionally, these CNCs are well-suited for multi-metal remediation systems and applications that necessitate food-contact safety, as they demonstrate biocompatibility.

Table 5. Removal Amount of Heavy Metals in 1 g of Adsorbent at Equilibrium Contact Time of 1.0 h, pH = 5, and Initial Concentration of 50 ppm

	Cu^{2+}			Cd^{2+}		
Name	AC (mg/g)	AE (%)	FC (ppm)	AC	AE	FC
Potato Pulp	3.56±0.1	51.4±0.1	24.38±0.1	3.98±0.1	73.7±0.1	13.15±0.2
Cellulose	2.99±0.1	49.9±0.0	25.03±0.1	3.31±0.1	66.26±0.2	16.87±0.2
CNCs	4.78±0.1	55.7±0.1	22.15±0.1	5.95±0.2	79.0±0.2	10.5±0.9

	Pb^{2+}		
Name	AC	AE	FC
Potato Pulp	5.93±0.0	78.64±0.1	10.68±0.2
Cellulose	5.29±0.1	75.96±0.1	12.02±0.1
CNCs	7.15±0.1	83.7±0.1	8.15±0.0

AC = Absorption capacity, RE = Removal efficiency, FC = Final concentration of heavy metal

These findings highlight the crucial role of feedstock selection in the formulation of cellulose-based adsorbents. Potato pulp presents distinct advantages over traditional sources, evidenced by a 33% reduction in hydrolysis time. Future research should focus on evaluating fixed-bed column performance, exploring regeneration cycles, and assessing the effects of real wastewater matrices. This comprehensive investigation delineates structure-property relationships that can inform the design of advanced biosorbents derived from agricultural byproducts.

Table 6. Comparison of Heavy Metal Adsorption Capacities of Nanocellulose from Various Sources

Feedstock Source	Typical Dimensions (L × W, nm)	Crystal-linity Index (%)	T^0_{onest} (^{0}C)	Pb^{2+} AC (mg/g)	Key Advantages / Notes	Reference
Potato Pulp	150 ± 40 × 10 ± 3	73.4	315.2	7.15	Low lignin, high sulfation, superior biocompatibility (>2000 µg/mL), simplified process.	This study
Potato Peel	100-200 × 5-15	70 - 75	290 - 300	~5.2	Well-established feedstock, readily available.	(Chen *et al*. 2012; Murayama *et al*. 2023)
Potato Peel	N.R.	N.R.	N.R.	~217	Very high capacity, specialized functionality. Requires intensive chemical post-modification.	(DWT 2021)
Wheat Bran	200-400 × 15-30	70.3	~280	7.56	Good adsorption capacity, common agro-waste.	(Xiao *et al*. 2019)
Garlic Straw	255 × 11	68.8	~220	N.R.	Good crystallinity, moderate thermal stability.	(Kallel *et al*. 2016)
Phragmites australis	N.R.	N.R.	N.R.	17.2	Excellent adsorption capacity, often requires multi-step process.	Gao *et al*. 2018)

N.R.: Not Reported in the cited source.

CONCLUSIONS

1. This study successfully demonstrated the isolation of cellulose nanocrystals (CNCs) from potato pulp, achieving a cellulose content of 92.6% and a crystallinity index of 73.4%.
2. The derived CNCs exhibited superior thermal stability, water/oil absorption capacities, and heavy metal adsorption efficiency, making them suitable for diverse applications.
3. Cytotoxicity tests confirmed the biocompatibility of the CNCs at concentrations up to 2000 µg/mL, highlighting their potential for biomedical and food packaging uses.
4. The valorization of potato pulp not only addresses waste management challenges but also provides a sustainable alternative to conventional CNCs sources, contributing to the development of a circular bioeconomy.

Funding Declaration

This research received funding from the Iran National Science Foundation (INSF) under Grant No. 99026654.

Data Availability Declaration

The data supporting the findings of this study are available from the corresponding author upon reasonable request.

Competing Interest Declaration

The authors declare that they have no known competing financial interests or personal relationships that could have appeared to influence the work reported in this paper.

REFERENCES CITED

Alemdar, A., and Sain, M. (2008). "Isolation and characterization of nanofibers from agricultural residues–Wheat straw and soy hulls," *Bioresour. Technol.* 99(6), 1664-1671. https://doi.org/10.1016/j.biortech.2007.04.029

Ammar, Z., Adly, M., Abdalakrim, S. Y. H., and Mehanny, S. (2024). "Incorporating date palm fibers for sustainable friction composites in vehicle brakes," *Sci. Rep.* 14(1), article 23204. https://doi.org/10.1038/s41598-024-73818-6

Asmi, R., and Divoux, T. (2018). "Rheo-electrical properties of carbon black gels in aqueous solution of carboxymethyl cellulose," in: *Research Report*, ESPCI Paris.

Bondeson, D., Mathew, A., and Oksman, K. (2006). "Optimization of the isolation of nanocrystals from microcrystalline cellulose by acid hydrolysis," *Cellulose* 13(2), 171-180. https://doi.org/10.1007/s10570-006-9061-4

Brinchi, L., Cotana, F., Fortunati, E., and Kenny, J. M. (2013). "Production of nanocrystalline cellulose from lignocellulosic biomass: technology and applications," *Carbohyd Polym.* 94(1), 154-169. https://doi.org/10.1016/j.carbpol.2013.01.033

Chen, D., Lawton, D., Thompson, M., and Liu, Q. (2012). "Biocomposites reinforced with cellulose nanocrystals derived from potato peel waste," *Carbohyd Polym.* 90(1), 709-716. https://doi.org/10.1016/j.carbpol.2012.05.055

Chen, W., Yu, H., and Liu, Y. (2011). "Preparation of millimeter-long cellulose I nanofibers with diameters of 30–80 nm from bamboo fibers," *Carbohyd. Polym.* 86(2), 453-461. https://doi.org/10.1016/j.carbpol.2011.04.061

de Oliveira, F. B., Bras, J., Pimenta, M. T. B., da Silva Curvelo, A. A., and Belgacem, M. N. (2016). "Production of cellulose nanocrystals from sugarcane bagasse fibers and pith," *Ind. Crop. Prod.* 93, 48-57. https://doi.org/10.1016/j.indcrop.2016.02.015

Dowlatshahi, S., Haratinezhad Torbati, A. R., and Loloei, M. (2014). "Adsorption of copper, lead and cadmium from aqueous solutions by activated carbon prepared from saffron leaves," *Environ. Health Eng. Manag.* 1(1), 37-44.

Gao, H., Duan, B., Lu, A., Deng, H., Du, Y., Shi, X., and Zhang, L. (2018). "Fabrication of cellulose nanofibers from waste brown algae and their potential application as milk thickeners," *Food Hydrocolloid.* 79, 473-481. https://doi.org/10.1016/j.foodhyd.2017.12.029

Goering, H. K., and Van Soest, P. J. (1970). *Forage Fiber Analyses (Apparatus, Reagents, Procedures, and Some Applications)*, Agriculture Handbook No. 379, ARS-USDA, Washington, D.C.

Govil, T., Wang, J., Samanta, D., David, A., Tripathi, A., Rauniyar, S., Salem, D. R., and Sani, R. K. (2020). "Lignocellulosic feedstock: A review of a sustainable platform for cleaner production of nature's plastics," *J. Clean. Prod.* 270, article 122521. https://doi.org/10.1016/j.jclepro.2020.122521

Hemida, M. H., Moustafa, H., Mehanny, S., Morsy, M., Abd EL Rahman, E. N., and Ibrahim, M. M. (2024). "Valorization of *Eichhornia crassipes* for the production of cellulose nanocrystals further investigation of plethoric biobased resource," *Sci. Rep.* 14(1), article 12387. https://doi.org/10.1038/s41598-024-63164-z

Hivechi, A., Bahrami, S. H., and Siegel, R. A. (2019). "Drug release and biodegradability of electrospun cellulose nanocrystal reinforced polycaprolactone," *Mater. Sci. Eng. C* 94, 929-937. https://doi.org/10.1016/j.msec.2018.10.037

Huang, L., Wang, K., Liu, H., and Lu, C. (2023). "Isolation and characterization of nanocellulose from sugarcane bagasse and its application in chicken meat preservation," *Food Chemistry*. 413, article 135675. https://doi.org/10.1016/j.foodchem.2023.135675

Jung, S.-J., Kim, S.-H., and Chung, I.-M. (2015). "Comparison of lignin, cellulose, and hemicellulose contents for biofuels utilization among 4 types of lignocellulosic crops," *Biomass Bioenerg.* 83, 322-327. https://doi.org/0.1016/j.biombioe.2015.10.007

Kallel, F., Bettaieb, F., Khiari, R., García, A., Bras, J., and Chaabouni, S. E. (2016). "Isolation and structural characterization of cellulose nanocrystals extracted from garlic straw residues," *Ind. Crop. Prod.* 87, 287-296. https://doi.org/10.1016/j.indcrop.2016.04.060

Kian, L. K., Jawaid, M., Ariffin, H., and Karim, Z. (2018). "Isolation and characterization of nanocrystalline cellulose from roselle-derived microcrystalline cellulose," *Int. J. Biol. Macromol.* 114, 54-63. https://doi.org/10.1016/j.ijbiomac.2018.03.065.

Li, M., Wang, L.-j., Li, D., Cheng, Y.-L., and Adhikari, B. (2014). "Preparation and characterization of cellulose nanofibers from de-pectinated sugar beet pulp," *Carbohyd. Polym.* 102, 136-143. https://doi.org/10.1016/j.carbpol.2013.11.021

Li, R., Fei, J., Cai, Y., Li, Y., Feng, J., and Yao, J. (2009). "Cellulose whiskers extracted from mulberry: A novel biomass production," *Carbohyd. Polym.* 76(1), 94-99. https://doi.org/10.1016/j.carbpol.2008.09.034

Lu, H., Gui, Y., Zheng, L., and Liu, X. (2013). "Morphological, crystalline, thermal and physicochemical properties of cellulose nanocrystals obtained from sweet potato residue," *Food Res. Int.* 50(1), 121-128. https://doi.org/10.1016/j.foodres.2012.10.013

Masood, H., Ullah, S., Ullah, Z., Irfan, M., Alam, O., Ali, M., Ismat, A., Khan, H., Haq, S., Ahmed, N., and Hameed, S. (2023). "Valorization of miscanthus stem waste for the production of cellulose nanofibers and their application in PLA composite for packaging," *Applied Nanoscience* 13(6), 4455-4469. https://doi.org/10.1007/s13204-022-02714-0

Mohammadpanah, F., Behrooz, R., Pooyan, M., Gholivand, K., and Roohzadeh, R. (2025). "Development of a phosphoaminopyrazine-loaded cellulose nanoparticle drug delivery system for targeted treatment of triple-negative breast cancer," *Int. J. Biol. Macromol.* 300, article 140206. https://doi.org/10.1016/j.ijbiomac.2024.140206

Mohammadpanah, F., Behrooz, R., and Roohzadeh, R. (2025). "Preparation and characterisation of water dispersible cellulose nanocrystals (CNC) dry powder from potato waste pulp of the potato starch industry: effect of drying method," *Bioresource Technology Reports* 2025, article 102311. https://doi.org/10.1016/j.biteb.2025.102311

Mu, R., Hong, X., Ni, Y., Li, Y., Pang, J., Wang, Q., Xiao, J., and Zheng, Y. (2020). "Recent trends and applications of cellulose nanocrystals in food industry," *Carbohydrate Polymers* 230, article 115676. https://doi.org/10.1016/j.carbpol.2019.115676

Murayama, D., Rankin, S. A., and Ikeda, S. (2023). "Bile salt-induced competitive displacement of cellulose nanocrystals from oil droplet surfaces," *Food Biophys.* 18(1), 48-57. https://doi.org/10.1007/s11483-022-09751-w

Olad, A., Doustdar, F., and Gharekhani, H. (2020). "Fabrication and characterization of a starch-based superabsorbent hydrogel composite reinforced with cellulose nanocrystals from potato peel waste," *Colloid. Surface. A* 601, article 124962. https://doi.org/10.1016/j.colsurfa.2020.124962

Pagnanelli, F., Mainelli, S., De Angelis, S., and Toro, L. (2005). "Biosorption of protons and heavy metals onto olive pomace: Modelling of competition effects," *Water Res.* 39(8), 1639-1651. https://doi.org/10.1016/j.watres.2005.01.023

Pandey, S. (2008). *Potato Research Priorities in Asia and the Pacific Region*, RAP Publication (FAO), Bangkok, Thailand

Pelegrini, B. L., Ré, F., de Oliveira, M. M., Fernandes, T., de Oliveira, J. H., Oliveira Junior, A. G., Girotto, E. M., Nakamura, C., Sampaio, A. R., and Valim, A. (2019). "Cellulose nanocrystals as a sustainable raw material: Cytotoxicity and applications on healthcare technology," *Macromol. Mater. Eng.* 304(8), article 1900092. https://doi.org/10.1002/mame.201900092

Rai, A. K., Al Makishah, N. H., Wen, Z., Gupta, G., Pandit, S., and Prasad, R. (2022). "Recent developments in lignocellulosic biofuels, a renewable source of bioenergy," *Fermentation* 8(4), article 161. DOI: 10.3390/fermentation8040161

Raigond, P., Raigond, B., Kochhar, T., Sood, A., and Singh, B. (2018). "Conversion of potato starch and peel waste to high value nanocrystals," *Potato Res.* 61(4), 341-351. https://doi.org/10.1007/s11540-018-9384-1

Rodrigues, R. C., Rodrigues, B. G., Canettieri, E. V., Martinez, E. A., Palladino, F., Wisniewski Jr, A., and Rodrigues Jr, D. (2022). "Comprehensive approach of methods for microstructural analysis and analytical tools in lignocellulosic biomass assessment – A review," *Bioresour. Technol.* 348, article 126627. https://doi.org/10.1016/j.biortech.2022.126627

Rupérez, P., and Saura-Calixto, F. (2001). "Dietary fibre and physicochemical properties of edible Spanish seaweeds," *Eur. Food Res. Technol.* 212(3), 349-354. https://doi.org/10.1007/s002170000264

Sadeghi-Shapourabadi, M., Elkoun, S., and Robert, M. (2023). "Microwave-assisted chemical purification and ultrasonication for extraction of nano-fibrillated cellulose from potato peel waste," *Macromol.* 3(4), 766-781. https://doi.org/10.3390/macromol3040044

Sain, M., and Panthapulakkal, S. (2006). "Bioprocess preparation of wheat straw fibers and their characterization," *Ind. Crop. Prod.* 23(1), 1-8. https://doi.org/10.1016/j.indcrop.2005.01.006

Schiewer, S., and Balaria, A. (2009). "Biosorption of Pb^{2+} by original and protonated citrus peels: Equilibrium, kinetics, and mechanism," *Chem. Eng. J.* 146(2), 211-219. https://doi.org/10.1016/j.cej.2008.09.005

Serpa, A., Velásquez-Cock, J., Gañán, P., Castro, C., Vélez, L., and Zuluaga, R. (2016). "Vegetable nanocellulose in food science: A review," *Food Hydrocolloid.* 57, 178-186. https://doi.org/10.1016/j.foodhyd.2016.01.023

Shojaeiarani, J., Bajwa, D.S., and Hartman, K. (2019). "Esterified cellulose nanocrystals as reinforcing filler for poly(lactic acid) nanocomposite films," *International Journal of Polymer Science* 2019, article 1767028. https://doi.org/10.1155/2019/1767028

Shruthy, R., Jancy, S., and Preetha, R. (2021). "Cellulose nanoparticles synthesised from potato peel for the development of active packaging film for enhancement of shelf life of raw prawns (*Penaeus monodon*) during frozen storage," *Int. J. Food Sci. Technol.* 56(8), 3991-3999. https://doi.org/10.1111/ijfs.15019

Sun, R., Tomkinson, J., Wang, Y., and Xiao, B. (2000). "Physico-chemical and structural characterization of hemicelluloses from wheat straw by alkaline peroxide extraction," *Polymer* 41(7), 2647-2656. https://doi.org/ 10.1016/S0032-3861(99)00436-X

Tibolla, H., Pelissari, F. M., Martins, J. T., Lanzoni, E. M., and Menegalli, F. C. (2018). "Banana starch nanocomposite with cellulose nanofibers isolated from banana peel by enzymatic treatment: In vitro cytotoxicity assessment," *Carbohyd. Polym* 207, 169-179. https://doi.org/10.1016/j.carbpol.2018.11.029

Tshikovhi, A., Mishra, S. B., and Mishra, A. K. (2023). "Lignocellulosic biomass-derived nanocellulose crystals as fillers in membranes for water and wastewater treatment: A review," *Cellulose* 30(18), 11473-11491. https://doi.org/10.1007/s10570-023-05560-7

Väisänen, T., Haapala, A., Lappalainen, R., and Tomppo, L. (2016). "Utilization of agricultural and forest industry waste and residues in natural fiber-polymer composites: A review," *Waste Manage.* 54, 62-73. https://doi.org/10.1016/j.wasman.2016.04.037

Ventura, C., Pinto, F., Lourenço, A. F., Ferreira, P. J., Louro, H., and Silva, M. J. (2020). "On the toxicity of cellulose nanocrystals and nanofibrils in animal and cellular models," *Cellulose* 27(10), 5509-5544. https://doi.org/10.1007/s10570-020-03176-9

Xiao, B., Sun, X., and Sun, R. (2001). "Chemical, structural, and thermal characterizations of alkali-soluble lignins and hemicelluloses, and cellulose from maize stems, rye straw, and rice straw," *Polym. Degrad. Stabil.* 74(2), 307-319. https://doi.org/10.1016/S0141-3910(01)00163-X

Xiao, Y., Liu, Y., Wang, X., Li, M., Lei, H., and Xu, H. (2019). "Cellulose nanocrystals prepared from wheat bran: Characterization and cytotoxicity assessment," *Int. J. Biol. Macromol.* 140, 225-233. https://doi.org/10.1016/j.ijbiomac.2019.08.160

Yang, H., Yan, R., Chen, H., Lee, D. H., and Zheng, C. (2007). "Characteristics of hemicellulose, cellulose and lignin pyrolysis," *Fuel* 86(12-13), 1781-1788. https://doi.org/10.1016/j.fuel.2006.12.013

Yousefi, H., Faezipour, M., Nishino, T., Shakeri, A., and Ebrahimi, G. (2011). "All-cellulose composite and nanocomposite made from partially dissolved micro-and nanofibers of canola straw," *Polym. J.* 43(6), 559-564. https://doi.org/10.1038/pj.2011.31

Zheng, Y., and Li, Y. (2018). "Physicochemical and functional properties of coconut (*Cocos nucifera* L) cake dietary fibres: Effects of cellulase hydrolysis, acid treatment and particle size distribution," *Food Chem.* 257, 135-142. https://doi.org/10.1016/j.foodchem.2018.03.012

Zhu, S., Sun, H., Mu, T., Li, Q., and Richel, A. (2023). "Preparation of cellulose nanocrystals from purple sweet potato peels by ultrasound-assisted maleic acid hydrolysis," *Food Chem.* 403, 134496. https://doi.org/10.1016/j.foodchem.2022.134496.

Article submitted: July 10, 2025; Peer review completed: November 30, 2025; Revised version received and accepted: January 26, 2026; Published: February 5, 2026.
DOI: 10.15376/biores.21.2.2851-2877